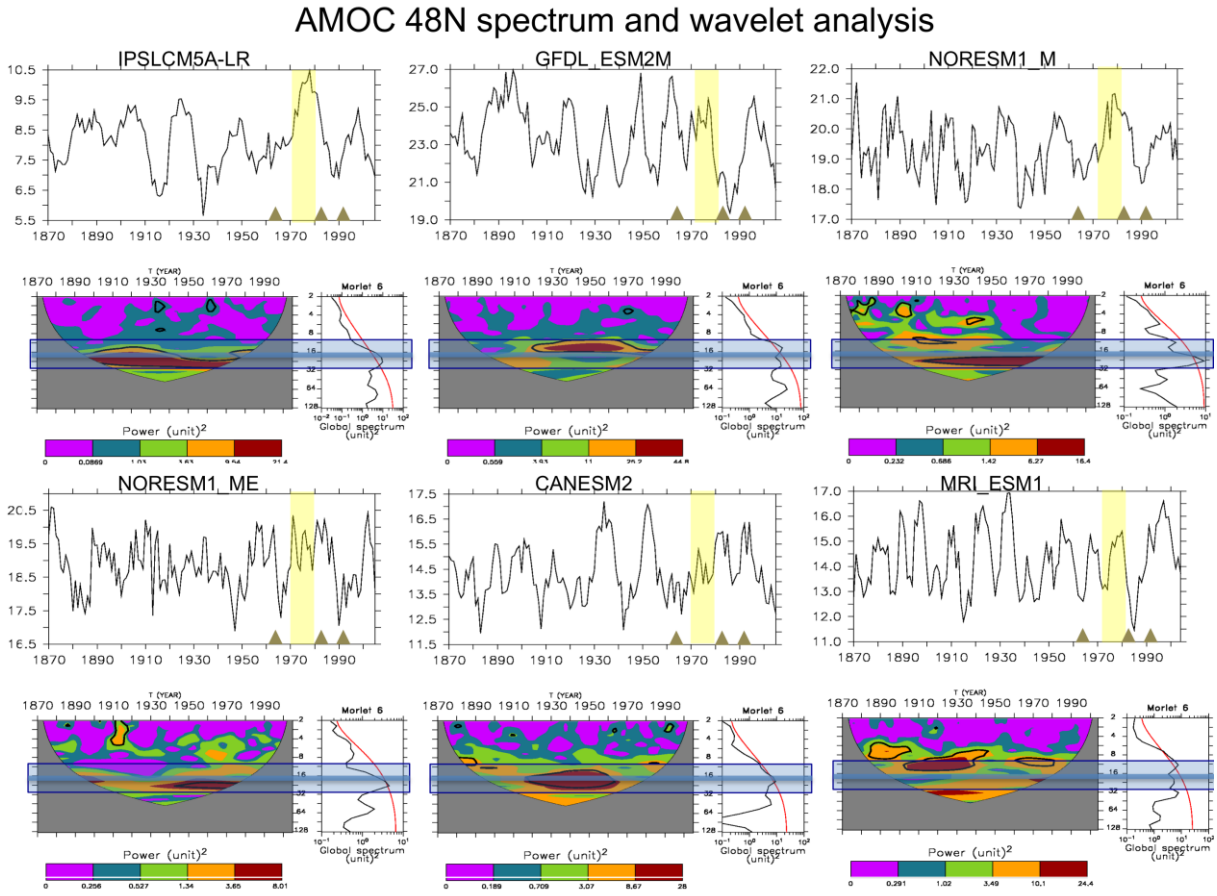

Supplementary Figure 1: **Time series of 48°N AMOC maximum from six model historical simulations based on different models**. For each model, the wavelet analysis of AMOC is also shown; bold contours mark significant energy peaks at the 95 % level, and the power spectrum of the AMOC (black) compared to an AR1 signal (red). We only show the subset of six models that exhibit larger energy than a red noise process in the spectral band 10-30 years (highlighted in blue) in their historical simulations. We also highlight the late 1970s maximum in yellow and the timing of the eruptions of the last 50 years with brown triangle.

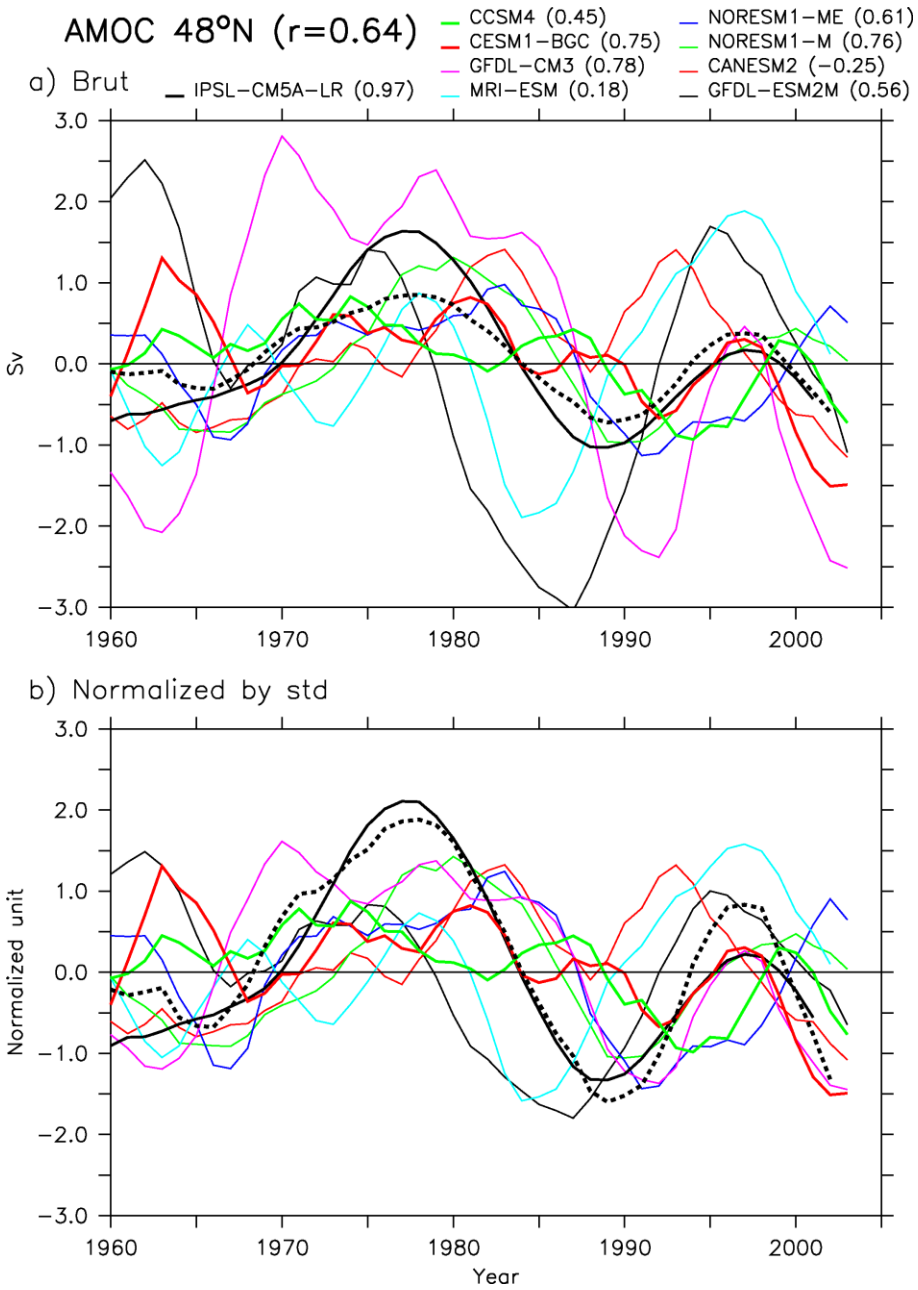

Supplementary Figure 2: **AMOC maximum at 48°N in the Bi-Dec subset of models**. In thick black is shown the ensemble mean of 5 historical simulations with IPSL-CM5A-LR and in thick dotted line is the Bi-Dec ensemble mean excluding IPSL-CM5A-LR. All datasets are shown smoothed with a 5-yr running mean. a) Data centred over their mean for the period 1950-2005 and b) same as a) but with data normalized with respect to their standard deviation over the same period. The numbers in parentheses in the legend correspond to the correlation of each member with the ensemble mean over the period 1970-2005.

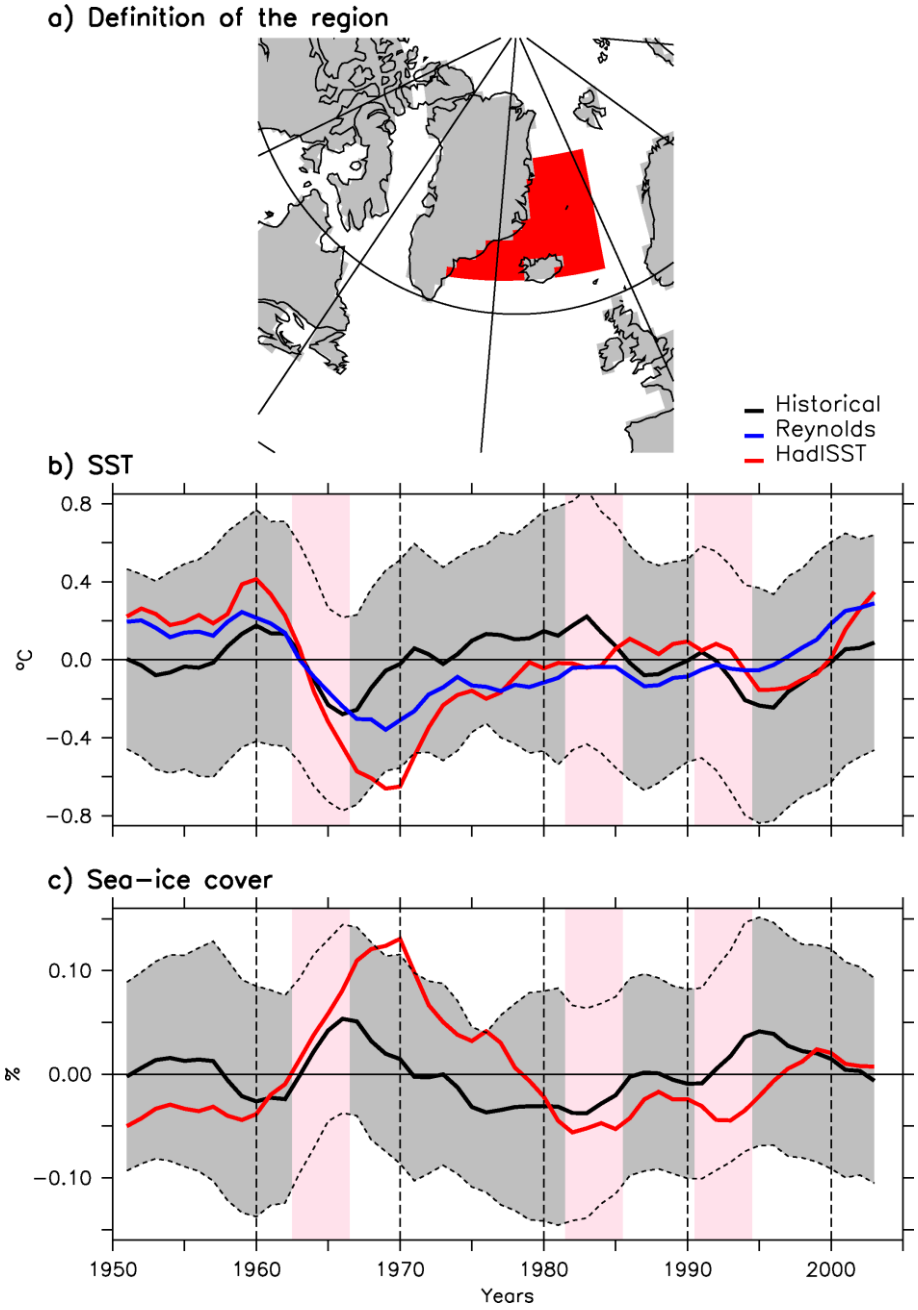

Supplementary Figure 3: **Time evolution over the red region** shown in panel a) of b) the SST and c) of the ice cover in the IPSL-CM5A-LR historical ensemble (black lines), the Reynolds et al. (2007) dataset[1] (in blue) and the HadISST dataset[2] (in red).

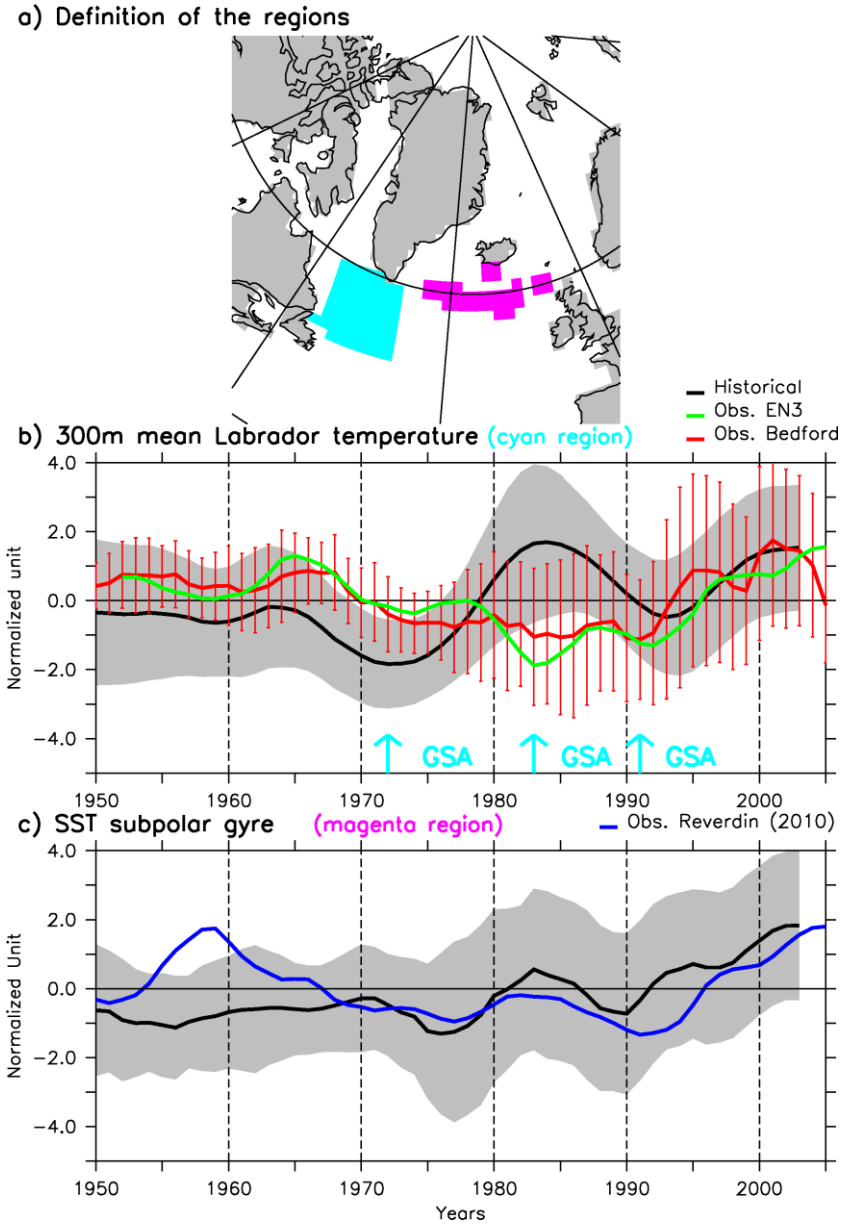

Supplementary Figure 4: **Observed and simulated changes in temperature**. a) Location of the two key regions (Labrador Sea and subpolar gyre) studied here. b) *In situ* temperature data from the Labrador Sea averaged over the cyan region down to 300m compiled from the Bedford Institute (*cf.* Methods, red line, with vertical line representing 2-standard deviation errors) and from EN3[3] (green) observational datasets. c) Sea Surface Temperature (SST) from *in situ* data[4] (in blue) averaged over the eastern subpolar gyre (magenta region). In panels b and c, the 5-member ensemble mean outputs from historical simulations using IPSL-CM5A-LR are also displayed (black, mean value; grey shaded, standard deviation envelope). The horizontal black lines at the top of panels b) and c) delimit the 20-year sliding windows for which significant correlation is detected (at the 95% confidence level) between the simulations and the observations (using the Bedford Institute data only in panel b). A 5-year running mean has been applied to all time series.

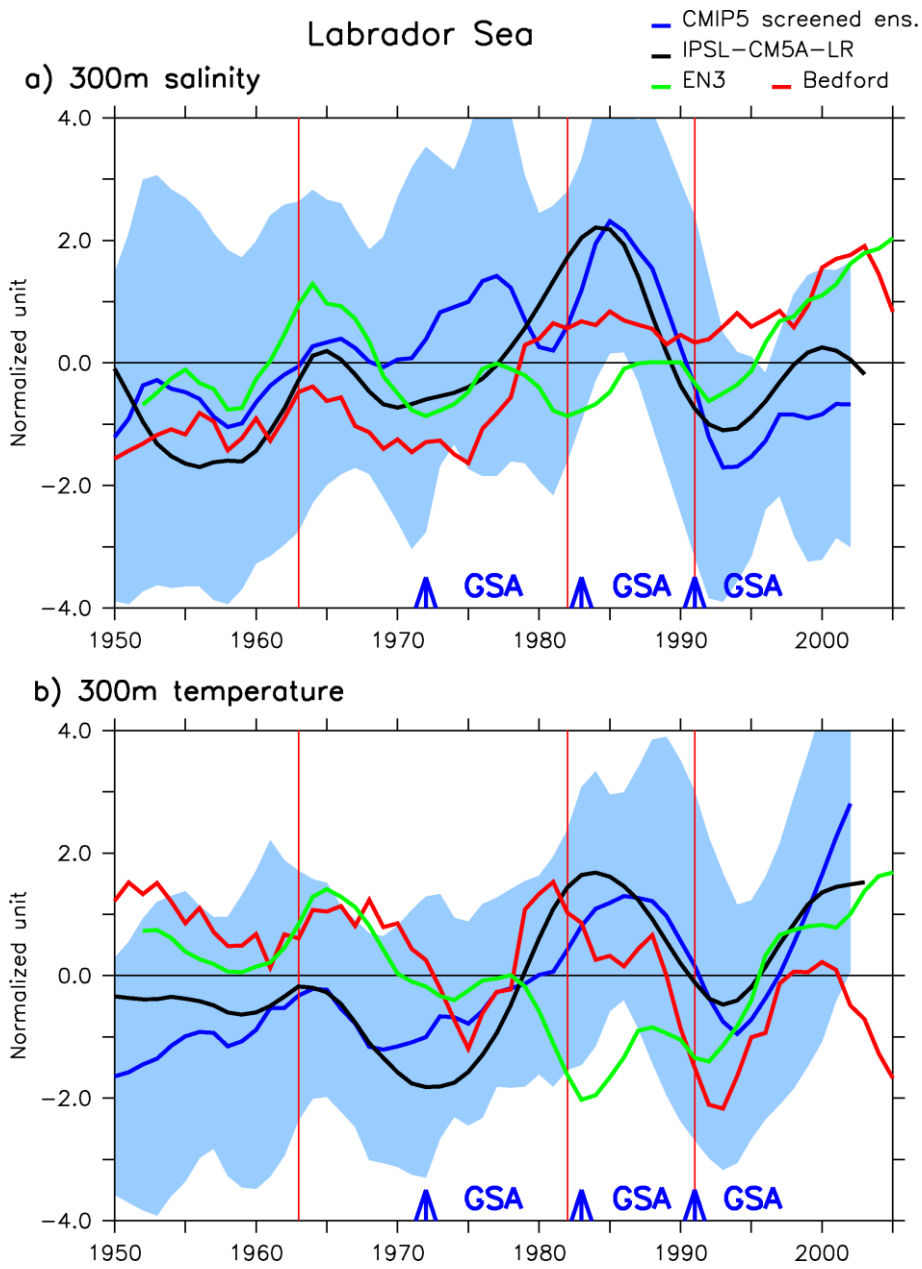

Supplementary Figure 5: **Observed and simulated changes in salinity.** *In situ* salinity data from the Labrador Sea averaged over wider area (65°W-40°W; 45°N-65°N) than in Figure 2b down to 300m compiled from the Bedford Institute (*cf.* Methods, red line) and from EN3[3] (green) observational datasets.. The blue line corresponds to the ensemble mean of the 8 screened models from CMIP5 ensemble (excluding IPSL-CM5A-LR) with their associated standard deviation. The black lines correspond to the ensemble mean historical simulations using IPSL-CM5A-LR. a) Salinity and b) temperature averaged over the first 300 meters.

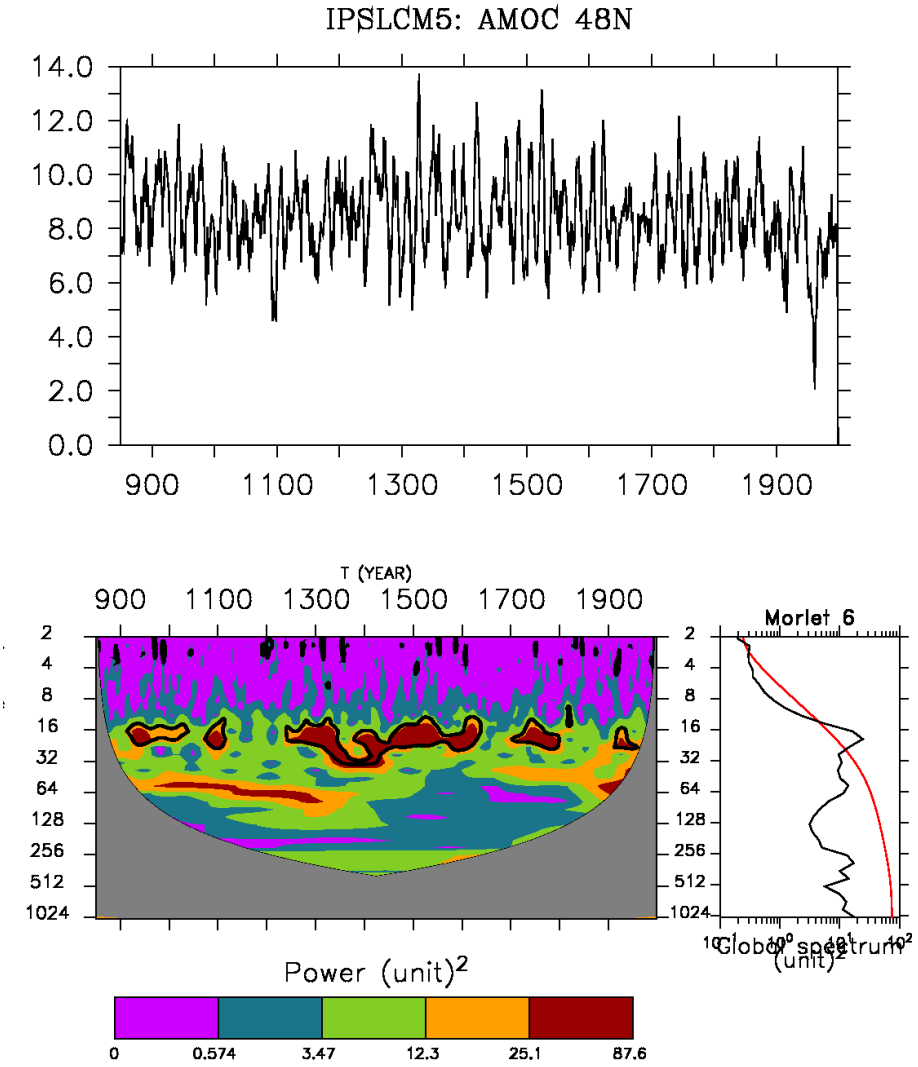

Supplementary Figure 6: **Wavelet analysis of the AMOC maximum at 48°N** from last millennium simulation using IPSL-CM5A-LR. The region significant at the 95 % level are marked using bold contours. Bottom right power spectrum of the signal in black compared to an AR1 signal.

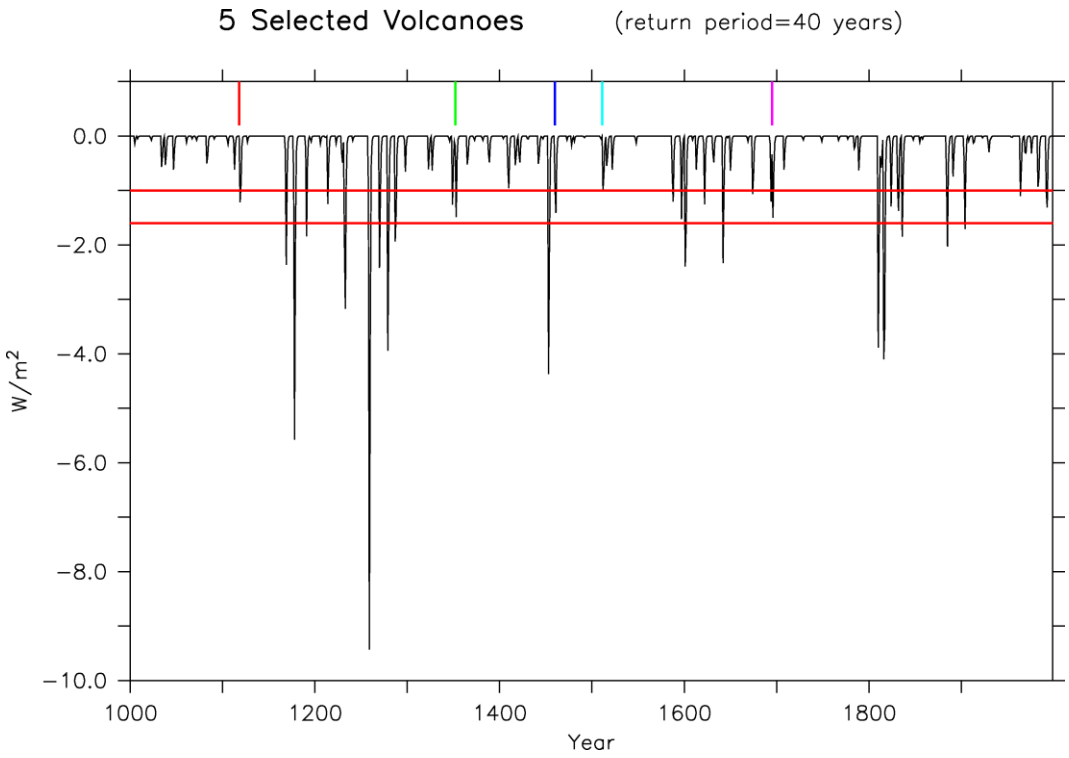

Supplementary Figure 7: **External forcing from volcanic eruption in the millennium simulation**. The coloured vertical bars at the top correspond to the volcanoes larger than 1963 Agung and lower than two times this eruption and without any subsequent large eruptions (larger radiative forcing than Agung) in the 40 following years. Following this method, we select 5 volcanoes between 1000 and 1850. The selected volcanoes have their maximum impact on the radiative forcing in 1118, 1352, 1460, 1511, 1695.

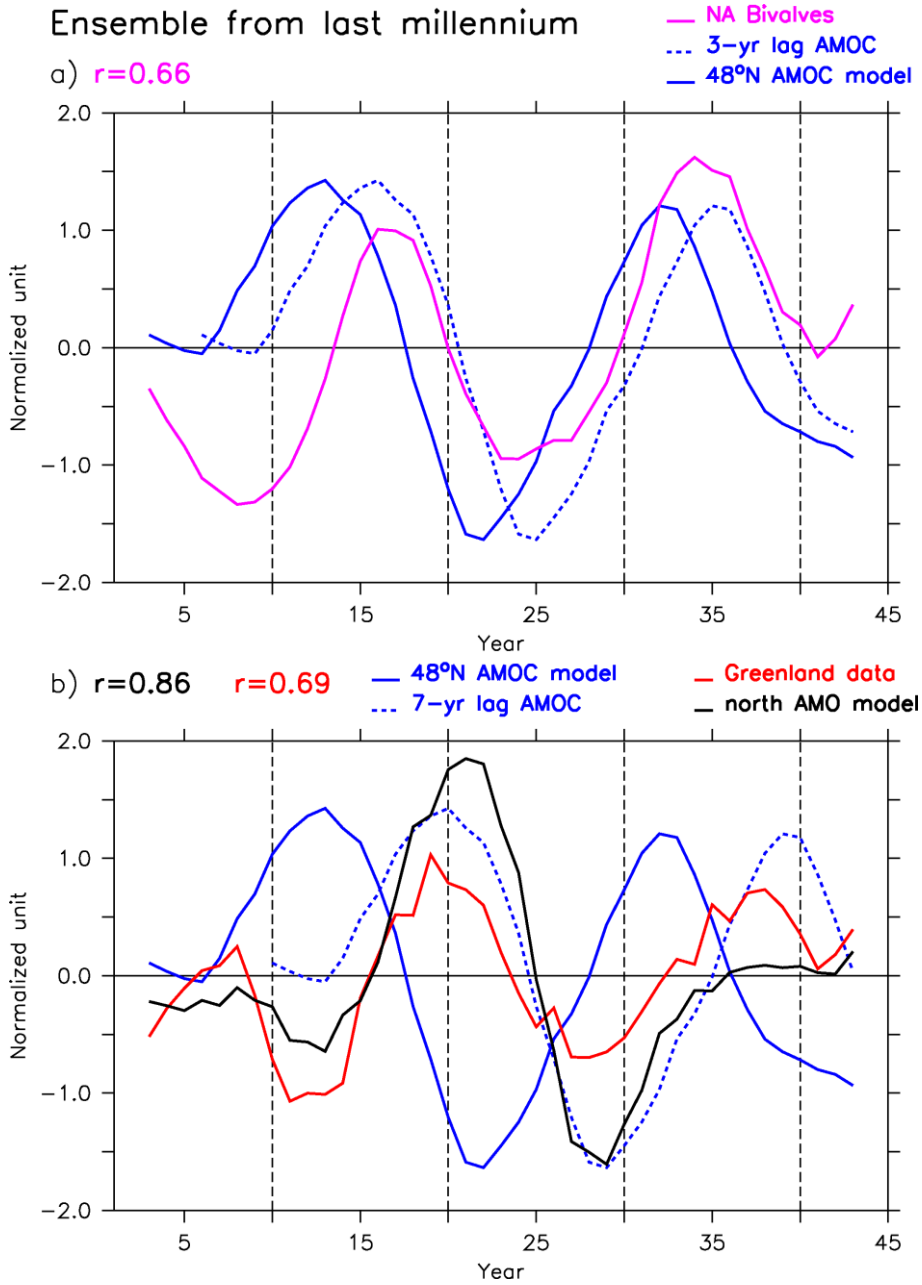

Supplementary Figure 8: a) Curves from Figure 6 shown on the same panel with in purple the bivalve data (purple) and in blue the modelled AMOC at 48°N (blue). The dotted blue line shows the AMOC with a 3-year time lag. The correlation between 3-year lagged AMOC and bivalve data equals 0.66, significant at the 95% level using a t-test to account for autocorrelation in the time series[5]. b) Curves from Figure 6 shown on the same panel with in red data from Greenland ice cores, in black north AMO from the model, in blue AMOC from the model at 48°N and in dotted blue 7-year lag AMOC. Correlation between 7-year lagged AMOC and Greenland data and north AMO equals 0.69 and 0.86 respectively, significant at the 95% level. A 5-year running mean has been applied to all time series.

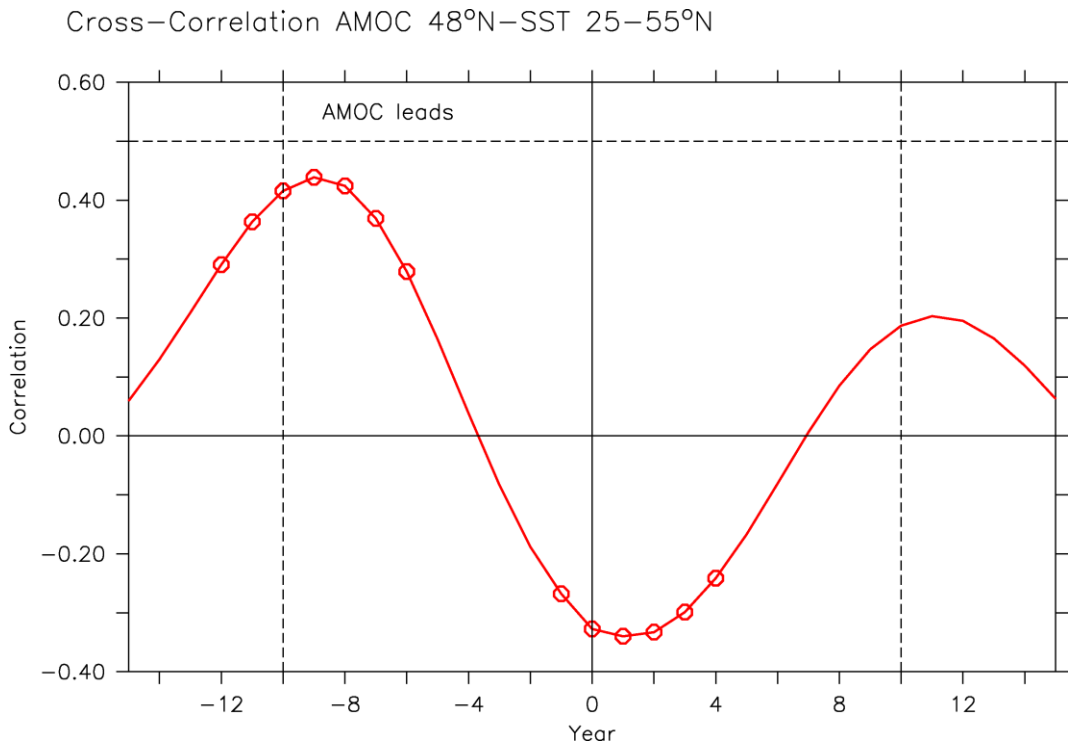

Supplementary Figure 9: **Cross-correlation between AMOC index at 48°N and SST** averaged in the Atlantic over the 25-55°N latitude band in the last millennium simulation computed over the time frame 850-1850. On the right (left) part of the graph, the AMOC is leading (lagging) the SST changes. The correlation coefficients statistically significant at the 95% level are highlighted with red circles.

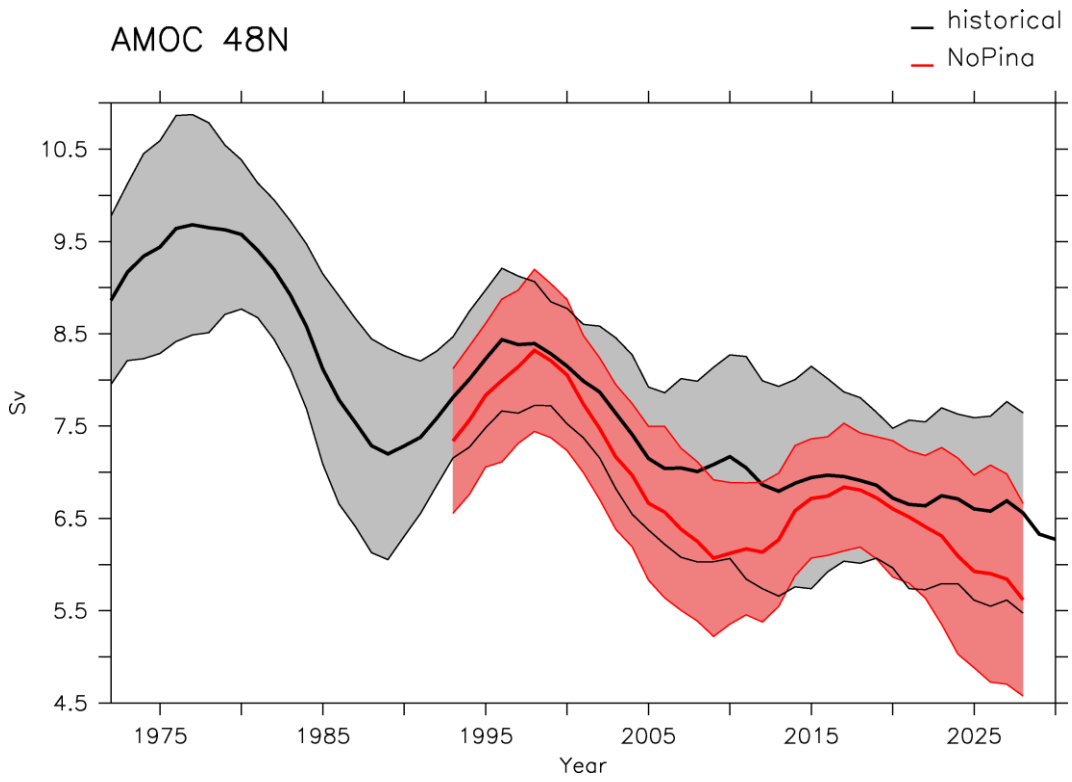

Supplementary Figure 10: **AMOC variations at 48°N** for the ensemble mean and standard deviation from the historical simulations in black and for the sensitivity experiments without Pinatubo eruptions in red.

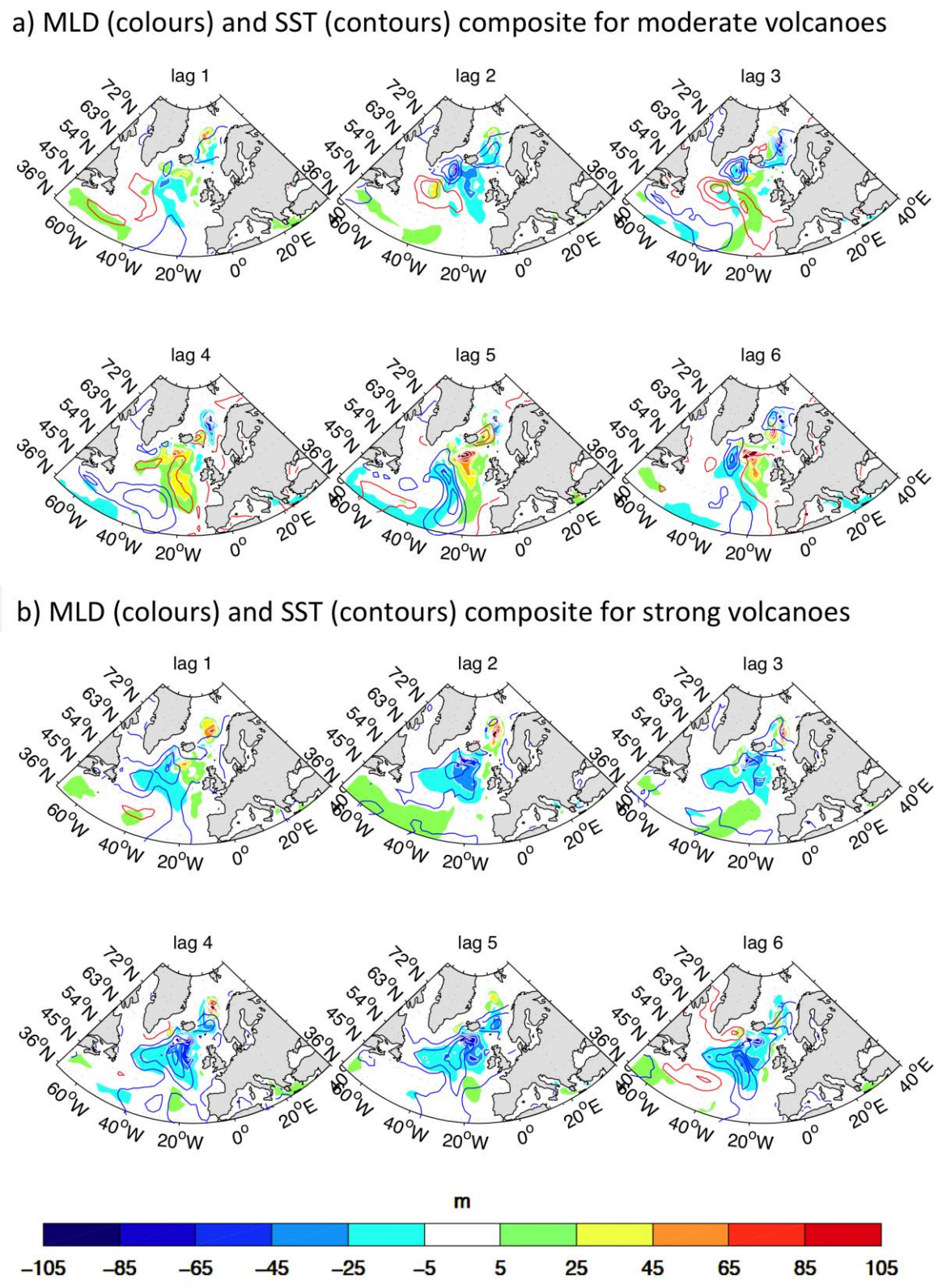

Supplementary Figure 11: Composite over moderate (lower than 1.5 Agung) and strong (larger than 1.5 Agung) volcanoes of the mixed layer depth (MLD) in colour and SST in contours computed within the last millennium simulation.

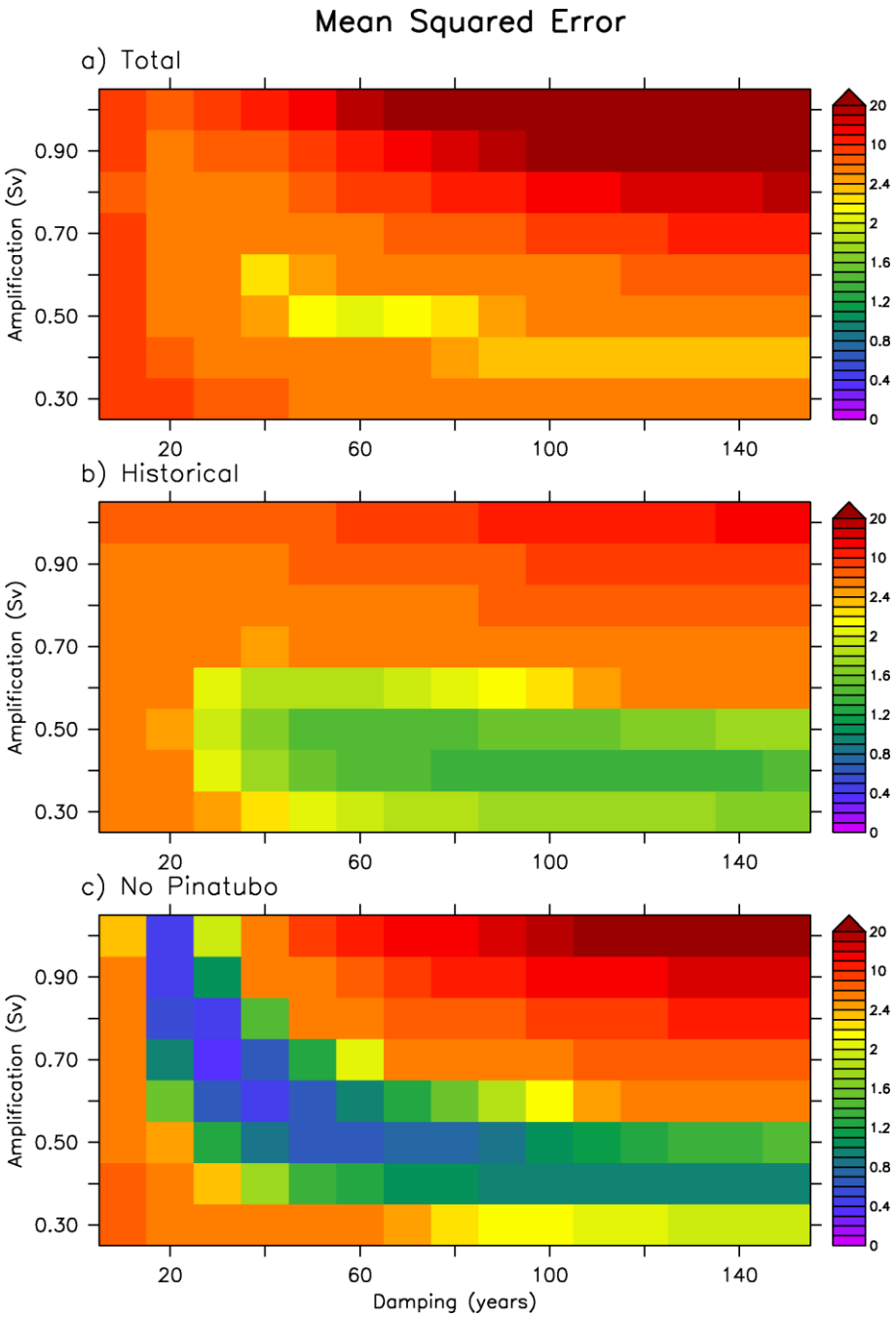

Supplementary Figure 12: Mean squared error between b) conceptual models and historical simulation computed over 1975-2030, c) conceptual models and simulation without Pinatubo computed over 1991-2030 and a) the sum of the two formers.

Supplementary Table 1: Table of the CMIP5 models analysed and summary of their main spectral characteristics deduced from spectral analysis illustrated in Supplementary Figure 1. The first column shows the model names, the second, the spectral characteristics of the pre-industrial simulations, the third gives the length of these simulations and the last column shows the spectral characteristic of historical simulations of 136 years long for all the models (1870-2005). The 9 models selected for the Bi-Dec ensemble are highlighted in bold in the table.

Models	**Frequency of AMOC variability**		
	pre-industrial		historical
	Preferential frequency	Length	Preferential frequency
ACCESS1-3	5-10 yrs	500 yrs	5-10 yrs
CanESM2	**5-15 yrs**	**1000 yrs**	**15-25 yrs**
CCSM4	**15-25 yrs**	**500 yrs**	**Mainly red**
CESM1-FASTCHEM	Mainly red	220 yrs	Mainly red
CESM1-CAM5	Mainly red	320 yrs	Mainly red
CESM1-WACCM	Mainly red	200 yrs	Mainly red
CESM1-BGC	**3yrs and 20-30 yrs**	**500 yrs**	**Mainly red**
CNRM-CM5	3 yrs and 100 yrs	850 yrs	Mainly red
FGOALS-g2	Mainly red	900 yrs	10 yrs
GFDL-CM3	**10-20 yrs**	**800 yrs**	**10-20 yrs**
GFDL-ESM2M	**3-5 yrs and 10-20 yrs**	**500 yrs**	**10-20 yrs**
inmcm4	Mainly red	500 yrs	Mainly red
IPSL-CM5A-LR	**15-25 yrs**	**1000 yrs**	**15-25 yrs**
IPSL-CM5B-LR	Mainly red	300 yrs	Mainly red
MPI-ESM-MR	Mainly red	1000 yrs	Mainly red
MPI-ESM-LR	5-10 yrs	1000 yrs	5-10 yrs
MRI-CGCM3	**5-15 yrs**	**500 yrs**	**5-15 yrs**
NorESM1-M	**15-25 yrs**	**500 yrs**	**15-25 yrs**
NorESM1-ME	**Mainly red**	**250 yrs**	**15-25 yrs**

Supplementary Table 2: list of IPSL-CM5A-LR simulations described in the text with their main characteristics (number of members, initial conditions, forcing used, restoring and length).

Name	# Ensemble	Initial conditions	Forcing	Restoring	Years of simulation
Control	1	Spin-up simulation	Pre-industrial	No	1x1000
Historical	5	Start in 1850 every 10 years from the pre-industrial simulation	Natural + Anthropogenic	No	5x156
No Pinatubo	5	Start in 1991 from each associated historical simulation	Natural + Anthropogenic – Pinatubo eruption	No	5x40
Nudged	5	Start in 1949 from each associated historical simulation	Natural + Anthropogenic	SST anomalies[1]	5x57
Millennium	1	Spin-up simulation	Natural + Anthropogenic	No	1x1150

Supplementary Table 3: Millennial-long Greenland ice cores used in the EOF analysis.

Site	Longitude	Latitude	Original Time Span	Reference
B18	-36.4	76.6	871-1992CE	From (Schwager 2000)[6, a]
Crete	-37.3	71.1	552-1973CE	From Vinther et al. (2010)[7, b]
DYE-3	-43.8	65.2	551-1978CE	From Vinther et al. (2010)[7, b]
GISP2	-38.5	72.6	818-1987CE	From Grootes and Stuiver (1997)[8, c]
GRIP	-37.6	72.6	551-1979CE	From Vinther et al. (2010)[7, b]
NGRIP	-42.3	75.1	1-1996CE	From Kaufman et al. (2009)[9, d]

[a] Data available in: http://doi.pangaea.de/10.1594/PANGAEA.57158?format=html

[b] Data available in: http://www.iceandclimate.nbi.ku.dk/data/Vinther_etal_2010_data_02feb2010.xls

[c] Data available in: ftp://ftp.ncdc.noaa.gov/pub/data/paleo/icecore/greenland/summit/gisp2/isotopes/d18o1yr.txt

[d] Data available in: http://www.iceandclimate.nbi.ku.dk/data/Kaufman_etal_2009_data_29sep2009.pdf

Supplementary References

1. Reynolds, R. *et al.* Daily high-resolution blended analyses for sea surface temperature. *J Clim* **20,** 5473–5496 (2007).

2. Rayner, N. a. Global analyses of sea surface temperature, sea ice, and night marine air temperature since the late nineteenth century. *J. Geophys. Res.* **108,** (2003).

3. Ingleby, B. & Huddleston, M. Quality control of ocean temperature and salinity profiles - Historical and real-time data. *J. Mar. Syst.* **65,** 158–175 (2007).

4. Reverdin, G. North Atlantic Subpolar Gyre Surface Variability (1895–2009). *J. Clim.* **23,** 4571–4584 (2010).

5. Bretherton, C., Widmann, M., Dymnikov, V., Wallace, J. & Blade, I. The Effective Number of Spatial Degrees of Freedom of a Time-Varying Field. *J. Clim.* **12,** 1990–2009 (1999).

6. Schwager, M. Ice core analysis on the spatial and temporal variability of temperature and precipitation during the Late Holocene in North Greenland. *Ber Polarforsch* **362,** (2000).

7. Vinther, B. *et al.* Climatic signals in multiple highly resolved stable isotope records from Greenland. *Quat. Sci Rev* **29,** 522–538 (2010).

8. Grootes, P. & Stuiver, M. Oxygen 18/16 variability in Greenland snow and ice with 10-3 to 105 year time resolution. *J Geophys Res* **102,** 26455–26470 (1997).

9. Kaufman, D. S. *et al.* Recent warming reverses long-term arctic cooling. *Science* **325,** 1236–1239 (2009).